Pentasaccharide Enhances the Inactivation of Factor Xa by Antithrombin by Promoting the Assembly of a Michaelis-Type Intermediate Complex. Demonstration by Rapid Kinetic, Surface Plasmon Resonance, and Competitive Binding Studies†

Alireza R. Rezaie*

Edward A. Doisy Department of Biochemistry and Molecular Biology, St. Louis University School of Medicine, St. Louis, Missouri 63104

Received January 10, 2006; Revised Manuscript Received March 1, 2006

ABSTRACT: It has been demonstrated that a unique pentasaccharide fragment of heparin (H5) activates AT by exposing an exosite on the serpin that is a recognition site for interaction with the basic autolysis loop (residues 143−154) of fXa. In support of this, the substitution of Arg-150 of fXa with Ala (R150A) impaired the reactivity of the mutant with AT by 1 order of magnitude specifically in the presence H5. To understand the mechanism by which heparin activation of AT improves the reactivity of the serpin with fXa, the H5-catalyzed reaction of AT with fXa, fXa R150A, and fXa S195A was studied using rapid kinetic, surface plasmon resonance, and competitive binding methods. The pseudo-first-order rate constants for the H5-catalyzed AT inhibition of both fXa and fXa R150A exhibited a linear dependence on the serpin concentration, thereby yielding second-order rate constants of 1.0×10^6 and 1.5×10^5 M^{-1} s^{-1}, respectively. On the other hand, an ∼70-saccharide, high-affinity heparin-catalyzed AT inhibition of both fXa derivatives showed a saturable dependence on the inhibitor concentration, yielding an identical rate constant of ∼20 s^{-1}, but different ternary fXa−heparin−AT dissociation constants ($K_{E,ATH}$) of ∼130 and ∼1780 nM for wild-type and R150A fXa, respectively. Competitive kinetic and surface plasmon resonance binding studies using the catalytically inactive S195A mutant of fXa yielded dissociation constants of 255 and 610 nM, respectively, for the mutant protease interaction with the AT−H5 complex. These results suggest that H5 enhances the reactivity of AT with fXa primarily by lowering the $K_{E,ATH}$ for the formation of a Michaelis-type serpin−protease encounter complex.

Antithrombin (AT)[1] is the primary serpin inhibitor in plasma that regulates the activities of the trypsin-like serine proteases of both the intrinsic and the extrinsic blood coagulation cascade (*1*−*5*). Like other inhibitory serpins, AT inactivates its target proteases by binding to their active sites through an exposed reactive center loop and undergoing a conformational change which traps the enzymes in inactive, stable complexes (*5*, *6*). However, AT is a slow inhibitor of coagulation proteases unless it binds to heparin-like glycosaminoglycans, similar to those found on the endothelium surface (*1*, *7*). A full-length heparin accelerates the inhibition of coagulation proteases by AT by 3−4 orders of magnitude; thus, the rate of protease inhibition by the serpin is only limited by diffusion (*3*, *8*). This is the basis for the extensive use of heparin for prophylaxis and treatment of venous thrombosis (*9*). In the case of fXa, the dramatic increase in the rate of protease inhibition by AT in the presence of heparin has been demonstrated to arise from (1) the ability of a unique pentasaccharide fragment of heparin to change the conformation of the serpin to facilitate its optimal recognition by the protease (activation mechanism) (*10*, *11*), and (2) the ability of a full-length heparin to bridge the serpin and enzyme in one complex in the presence of physiological concentrations of Ca^{2+}, thereby promoting the initial interaction between the two proteins (template mechanism) (*12*, *13*). It has been demonstrated that the cofactor effect of a full-length heparin (∼70 saccharides) accelerates the AT inhibition of fXa ∼300-fold through the activation of serpin (*10*) and ∼200−300-fold through a template mechanism in the presence of Ca^{2+} (*13*).

Previous rapid kinetic studies have indicated that AT inactivates fXa and other target coagulation proteases by a two-step reaction mechanism in which an initial Michaelis-type enzyme−inhibitor complex, formed in the first reaction step, is converted to an irreversible covalent complex in the second step of the reaction (*14*, *15*). The dissociation constant ($K_{E,AT}$) for formation of the initial noncovalent serpin−protease complex is very high for the reaction of AT with fXa (and other coagulation proteases) in the absence of

† The research discussed herein was supported by Grant HL-62565 from the National Heart, Lung, and Blood Institute of the National Institutes of Health.

* To whom correspondence should be addressed: Department of Biochemistry and Molecular Biology, St. Louis University School of Medicine, 1402 S. Grand Blvd., St. Louis, MO 63104. Phone: (314) 977-9240. Fax: (314) 977-9205. E-mail: rezaiear@slu.edu.

[1] Abbreviations: AT, antithrombin; fXa, active factor Xa; Gla, γ-carboxyglutamic acid; GD-fXa, Gla-domainless factor Xa, factor Xa from which amino-terminal residues 1−45 have been removed; GD-fXa S1950A, Gla-domainless factor Xa derivative in which the catalytic residue Ser-195 [in the chymotrypsin numbering system of Bode et al. (*16*)] has been substituted with Ala; fXa R150A, factor Xa mutant in which Arg-150 has been replaced with Ala; BSA, bovine serum albumin; PEG, polyethylene glycol.

10.1021/bi060056r CCC: $33.50
Published on Web 03/24/2006

heparin (*14*, *15*). A full-length heparin consisting of ~70 saccharides (H70) has been demonstrated to lower the dissociation constant for formation of the noncovalent serpin−protease complex by ~4−5 orders of magnitude with both fXa and thrombin at a physiological Ca^{2+} concentration, ionic strength, and pH (*13*). In the case of thrombin, it is well established that the heparin bridging of both the serpin and the protease in one complex is solely responsible for rate enhancement of the polysaccharide, which lowers the dissociation constant for formation of a noncovalent AT−thrombin encounter complex (*15*). Although the 200−300-fold rate accelerating effect of H70 in catalyzing the AT inhibition of fXa is also mediated via the polysaccharide lowering the dissociation constant for formation of the noncovalent serpin−protease encounter complex (*13*), the mechanism of the H5-mediated interaction of the activated AT with fXa is not known.

It has recently been demonstrated that Arg-150 of the autolysis loop of fXa [chymotrypsin numbering (*16*)] is a recognition site for specific interaction with the activated conformation of AT (*17*). The substitution of this residue with Ala has decreased the reactivity of the mutant protease with AT by 1 order of magnitude in the presence of H5 (*17*). The decrease in the reactivity of the fXa mutant with AT has been shown to be specific for the activated conformation of the serpin since the mutant protease reacted normally with the native conformation of the serpin (*17*). The important role of the autolysis loop of fXa in reaction with the activated conformation of AT has been confirmed by the observation that activated protein C and thrombin fusion mutants containing the autolysis loop of fXa both exhibited high reactivity with AT specifically in the presence of pentasaccharide (*18*). In the study presented here, rapid kinetic measurements of the H5- and H70-catalyzed reactions of AT with both wild-type and R150A fXa together with surface plasmon resonance and competitive binding methods have been employed to determine the mechanism by which activated AT effectively inhibits fXa.

MATERIALS AND METHODS

Preparation of Recombinant Proteins and Other Reagents. Construction and expression of the Arg-150 to Ala (R150A) substitution mutant of fX were previously described (*17*). Gla-domainless fX (GD-fX) and a mutant in which the catalytic Ser-195 residue has been replaced with Ala (S195A) were constructed by PCR mutagenesis methods and expressed in human embryonic kidney cells (293) using the RSV-PL4 expression/purification vector system as described previously (*19*). The fX derivatives were activated by the factor X-activating enzyme from Russell's viper venom (Haematologic Technologies Inc., Essex Junction, VT) and purified on a SBTI-agarose column as described previously (*20*). Human plasma fXa and AT were purchased from Enzyme Research Laboratories (South Bend, IN). Active site concentrations of fXa derivatives were determined by titrations with AT assuming a 1:1 stoichiometry (*13*). The therapeutic pentasaccharide fragment of heparins, fondaparinux sodium (H5, molecular mass of 1.728 kDa), was from Organon Sanofi-Synthelabo. The full-length high-affinity heparin containing ~70 saccharides (H70) isolated from commercial heparin by size and AT affinity fractionation was a generous gift from S. Olson of the University of Illinois (Chicago, IL). Concentrations of heparins were based on AT binding sites and were determined by stoichiometric titrations of AT with the polysaccharides, with monitoring of the interaction by changes in protein fluorescence as described (*21*). The chromogenic substrate Spectrozyme FXa (SpFXa, MeO-CO-D-Chg-Gly-Arg-pNA) was purchased from American Diagnostica (Greenwich, CT). Polybrene and the fluorogenic substrate *N*-t-Boc-Ile-Glu-Gly-Arg-7-amido-4-methylcoumarin (Boc-IEGR-amc) were purchased from Sigma (St. Louis, MO).

Kinetic Methods. The rate of inactivation of fXa derivatives by AT in both the absence and presence of H5 and H70 was measured under pseudo-first-order conditions by a discontinuous assay method as described previously (*13*). In the absence of heparin, 1 nM fXa was incubated with 250−1000 nM AT in 0.1 M NaCl and 0.02 M Tris-HCl (pH 7.5) (TBS buffer, ionic strength of 0.12) containing 2.5 mM $CaCl_2$ (TBS/Ca^{2+}), 0.1 mg/mL bovine serum albumin (BSA), and 0.1% polyethylene glycol (PEG) 8000. In the presence of H5, either wild-type or R150A fXa (0.5 nM) was incubated with 25−200 nM AT in the presence of excess H5 (1 μM) in the same buffer system. In the presence of H70, the experimental conditions were the same except that each protease was incubated with 200 nM AT and catalytic levels of heparin (1−10 nM). All reactions were carried out in 50 μL volumes in 96-well vinyl plates at room temperature. After a period of time (10 s to 10 min depending on the rate of the reactions), 50 μL of the chromogenic substrate (200 μM SpFXa) in TBS containing 0.1% PEG 8000 and 1 mg/mL polybrene was added to each well and the remaining enzyme activity was measured with a V_{max} kinetics microplate reader (Molecular Devices, Menlo Park, CA). The observed pseudo-first-order rate constants (k_{obs}) and the second-order association rate constants for uncatalyzed and catalyzed reactions were obtained as described previously (*13*). All values are the average of at least three independent measurements ± the standard deviation.

Rapid kinetic analysis was carried out to resolve the two-step reaction of the AT−heparin complex with wild-type and R150A fXa in TBS/Ca^{2+} containing 0.1% PEG 8000 at 25 °C. In this case, the inactivation reaction was followed by a continuous assay in an Applied Photophysics SX.18MV-R stopped-flow instrument using the fluorogenic substrate, Boc-IEGR-amc, as described previously (*13*). The excitation wavelength was set to 380 nm and fluorescence detected with a 420 nm emission cutoff filter. For the AT reactions in the presence of H70, AT concentrations ranged from 100 to 5000 nM, H70 concentrations from 5 to 4000 nM, and fXa derivative concentrations from 2 to 300 nM, and Boc-IEGR-amc was present at 50 or 100 μM. For the reactions in the presence of H5, AT concentrations ranged from 200 to 12 000 nM, H5 concentrations from 10 to 10 000 nM, and fXa derivative concentrations from 2 to 300 nM, and the substrate was present at 50 or 100 μM. Pseudo-first-order conditions were obtained by employing a >10-fold molar excess of AT−heparin complex over the enzymes. To maintain a relatively constant fluorescence amplitude in these reactions, the ratio of heparin to enzyme was kept constant. The k_{obs} values were determined by computer fitting of fluorescence progress curves to a single exponential with a linear end point equation. The dependence of k_{obs} (the average of 5−10 progress curves) on the AT−H70 complex con-

centration was computer fit by the hyperbolic eq 1 (*13*)

$$k_{obs} = (k_{lim}[\text{AT}-\text{heparin}]/K_{E,ATH})(1 + [S_o]/K_M) + [\text{AT}-\text{heparin}] \quad (1)$$

where k_{lim} represents the limiting rate constant for conversion of the intermediate AT−H70−fXa ternary encounter complex to a stable AT−fXa complex with release of heparin, [AT−heparin] is the concentration of the AT−heparin complex which was calculated on the basis of the dissociation constant for the AT−heparin interaction using the quadratic equation [fixed to values of 5 and 23 nM for H70 and H5, respectively (*13*)], $K_{E,ATH}$ is the dissociation constant for the Michaelis-type fXa−AT−heparin ternary complex, $[S_o]$ is the concentration of the fluorogenic substrate, and K_M is the Michaelis constant for substrate hydrolysis by the enzymes. In both cases, K_M was fixed at a measured value for fXa hydrolysis of 300 μM Boc-IEGR-amc in TBS buffer containing 2.5 mM Ca^{2+} as described previously (*13*). In the case of H5 where the dependence of k_{obs} on AT−H5 complex concentration was linear, the linear regression slope according to eq 2 provided the overall second-order rate constant ($k_{lim}/K_{E,ATH}$) after multiplying by the factor $1 + [S_o]/K_M$ to correct for the competitive effect of the fluorogenic substrate.

$$k_{obs} = (k_{lim}[\text{AT}-\text{heparin}]/K_{E,ATH})(1 + [S_o]/K_M) \quad (2)$$

Competitive Binding. The competitive effect of the catalytically inactive S195A mutant of GD-fXa on the wild-type GD-fXa inhibition by AT both in the absence and in the presence of H5 was studied using the same discontinuous assay described above. In this case, the inhibition of GD-fXa (1 nM) by AT (50 nM) was monitored in the presence of increasing concentrations of GD-fXa S195A (0−10 μM) in the absence and presence of a fixed concentration of H5 (25 nM) in TBS/Ca^{2+} containing 0.1 mg/mL BSA and 0.1% PEG 8000. Following incubation for 2−3 min at room temperature, 50 μL of SpFXa was added to each well and the remaining activity of GD-fXa was measured as described above. Under these experimental conditions, more than 90−95% of the enzyme activity in the absence of the competitor was inhibited. K_D for the noncovalent interaction of the activated conformation of AT with GD-fXa was determined from the nonlinear regression analysis of the saturable S195A concentration dependence for recovery of the enzyme activity monitored by the hydrolysis of SpFXa at 405 nm as described above.

Surface Plasmon Resonance (SPR). The interaction of AT with GD-fXa S195A immobilized on a dextran-coated CM5 sensor chip was analyzed by SPR using the BIAcore (Uppsala, Sweden) X biosensor instrument. The inactive fXa mutant was coupled to the CM5 sensor chip to obtain a resonance unit (RU) of ~500 using an amine coupling kit according to the manufacturer's instructions. The HBS buffer containing 10 mM HEPES (pH 7.4), 150 mM NaCl, 3.4 mM EDTA, and 0.005% surfactant P20 was used as the running buffer. For analysis of the binding interactions, human AT was diluted to different concentrations of 2.5−1280 nM in the same buffer containing 4 μM H5 and was injected into flow cell 2, housing the immobilized S195A GD-fXa sensor chip. The binding sensogram was generated with a flow rate of 40 μL/min with an injection time of 2 min. Under these conditions, an RU value of ~150 was obtained at the highest concentration of the serpin. Control experiments included injection of 1280 nM AT alone or 4 μM H5 alone in the same buffer for 2 min with the same flow rate. No regeneration step was necessary since the running buffer lacking H5 completely dissociated AT from the sensor chip as evidenced by RU returning to a zero baseline following the completion of sample injection. The flow cell 1 reference-deducted sensogram data output obtained with different concentrations of the AT−H5 complex was analyzed using BIAevaluation software provided by the manufacturer. The global fitting of the binding data to a 1:1 Langmuir binding model yielded rate constants for association (k_a) and dissociation (k_d) and the equilibrium dissociation constant (K_D) for the noncovalent interaction of AT with the inactive fXa mutant in the presence of pentasaccharide.

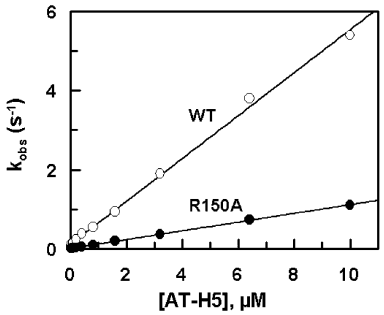

FIGURE 1: Dependence of k_{obs} for wild-type and R150A fXa inhibition on the AT−H5 complex concentration. The k_{obs} values were determined from the exponential decrease in the rate of hydrolysis of the fluorogenic substrate, Boc-IEGR-amc, due to inhibition of wild-type fXa (○) or R150A fXa (●) by the increasing concentrations of the AT−H5 complex (*x*-axis) in TBS/Ca^{2+} containing 0.1% PEG 8000. All reactions used a molar excess of AT over H5 to saturate the pentasaccharide, with exact concentrations of the AT−H5 complex calculated on the basis of the known dissociation constant for the interaction. The solid lines are least-squares computer fits of data by the linear eq 2 as described in Materials and Methods.

RESULTS AND DISCUSSION

AT inhibits fXa by a two-step reaction mechanism in which a noncovalent enzyme−inhibitor encounter complex, formed in the initial step, is converted to a stable covalent complex in the second step of the reaction (*14*). Rapid kinetic analysis was carried out to determine the step which was affected in the reaction of R150A fXa with AT in the presence of pentasaccharide. Under the experimental conditions described in the legend of Figure 1, the pseudo-first-order rate constant (k_{obs}) for inhibition of both wild-type and mutant fXa by the AT−H5 complex increased linearly, suggesting that the ternary dissociation constant ($K_{E,ATH}$) for formation of the intermediate noncovalent complex is higher than 10 μM. In this case, only second-order rate constants could be calculated from the slope of the linear dependence of k_{obs} values on the AT−H5 complex concentration according to eq 2 (Table 1). Since a full-length ~70-saccharide heparin (H70) has been demonstrated to decrease the $K_{E,ATH}$ value of the fXa−AT interaction to ~100 nM in the presence of a physiological concentration of Ca^{2+} (*13*), rapid kinetic analysis was also carried out using increasing concentrations of the AT−H70 complex in TBS containing 2.5 mM Ca^{2+}.

Table 1: Kinetic Constants for the Heparin-Catalyzed Reactions of AT with Wild-Type and R150A fXa As Measured by Continuous (stopped-flow) and Discontinuous (end point) Assay Methods

	heparin	$K_{E,ATH}$ ($\times 10^{-6}$ M)	k_{lim} (s^{-1})	k_2 ($\times 10^6$ M^{-1} s^{-1})
stopped-flow[a]				
fXa	H70	130 ± 20	19 ± 1	146 ± 30
fXa R150A	H70	1780 ± 260	21 ± 2	12 ± 3
fXa	H5	ND[c]	ND[c]	0.7 ± 0.01
fXa R150A	H5	ND[c]	ND[c]	0.1 ± 0.001
end point[b]				
fXa	H70	ND[c]	ND[c]	110 ± 10
fXa R150A	H70	ND[c]	ND[c]	15 ± 1
fXa	H5	ND[c]	ND[c]	1.0 ± 0.1
fXa R150A	H5	ND[c]	ND[c]	0.15 ± 0.02

[a] The kinetic constants were determined by rapid kinetic analyses of the observed pseudo-first-order rate constants (k_{obs}) for wild-type and R150A fXa inactivation by the AT−heparin complexes as a function of the AT−heparin complex concentrations in TBS buffer containing 0.1% PEG 8000 and 2.5 mM Ca^{2+}. AT−heparin complexes were formed by mixing full-length (H70) or pentasaccharide heparin (H5) with a molar excess of AT sufficient to saturate the polysaccharides. $K_{E,ATH}$ and k_{lim} values were obtained from computer fits of the saturable dependence of k_{obs} on the AT−heparin complex concentrations according to eq 1, after correction for the competitive effect of the reporter substrate as described in Materials and Methods. Overall second-order rate constants (k_2) were calculated from the $k_{lim}/K_{E,ATH}$ ratio or were determined from the slope of the linear regression line fitted to plots of k_{obs} vs AT−heparin complex concentration according to eq 2 after correction for substrate competition. [b] The heparin-catalyzed second-order association rate constants were determined from the residual chromogenic activities of fXa derivatives (0.5 nM) after incubation at room temperature with AT (25−200 nM) in complex with 1 μM H5 for 30 s in TBS buffer containing 0.1 mg/mL BSA, 0.1% PEG 8000, and 2.5 mM Ca^{2+}. The same methods were used to measure the k_2 values in the presence of H70 except that 0.5 nM enzyme was incubated with 1−10 nM heparin and 200 nM AT for 10−20 s. The second-order inactivation rate constants were calculated as described in Materials and Methods. [c] Could not be determined.

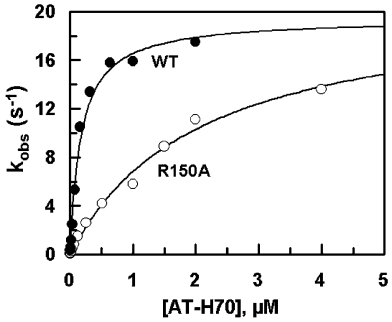

FIGURE 2: Dependence of k_{obs} for wild-type and R150A fXa inhibition on the AT−H70 complex concentration. The k_{obs} values for wild-type (●) and R150A fXa (○) inhibition by AT were determined for ~70-saccharide heparin-catalyzed reactions in TBS/Ca^{2+} containing 0.1% PEG 8000 as in Figure 1. The solid lines are least-squares computer fits of data to the hyperbolic eq 1 as described in Materials and Methods.

In this case, a saturable dependence of k_{obs} on the AT−H70 complex concentration was observed for both wild-type and mutant fXa (Figure 2), indicating the saturation of an intermediate heparin−AT−fXa encounter complex prior to formation of the stable serpin−protease complex. Nonlinear regression analysis of data by the hyperbolic eq 1 yielded values of 130 ± 20 nM for $K_{E,ATH}$ and 19 ± 1 s^{-1} for the limiting rate constant (k_{lim}) for formation of the stable complex of wild-type fXa and 1780 ± 260 nM for $K_{E,ATH}$ and 21 ± 2 s^{-1} for k_{lim} for the mutant protease (Table 1).

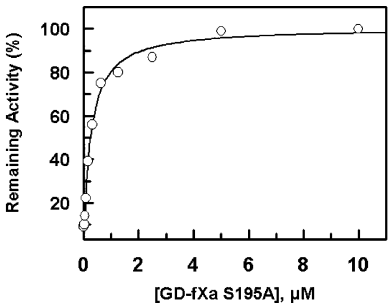

FIGURE 3: Competitive effect of inactive S195A GD-fXa on inhibition of wild-type GD-fXa by the AT−H5 complex. GD-fXa (1 nM) was incubated with 50 nM AT in complex with 25 nM H5 in TBS/Ca^{2+} containing 0.1 mg/mL BSA and 0.1% PEG 8000 at room temperature for 2.5 min followed by monitoring of the amidolytic activity of GD-fXa using Spectrozyme FXa as described in Materials and Methods.

These results indicate that the impairment in the reactivity of the fXa mutant with the H5-activated conformation of AT is localized to formation of the Michaelis-type noncovalent complex in the first reaction step. The calculated ratio of k_{lim} to $K_{E,ATH}$, corresponding to the overall second-order rate constant, agreed reasonably well with the directly determined value by a discontinuous assay and was 1 order of magnitude lower for the mutant than for wild-type fXa (Table 1). Noting that the lower reactivity of the fXa mutant with AT is specific for the activated conformation of AT (k_2 values of 3 × 10^3 and 2 × 10^3 M^{-1} s^{-1} were obtained for wild-type and mutant fXa reactions with AT in the absence of heparin, respectively), we show these results indicate that the stimulating effect of H5 on AT inhibition of fXa is primarily due to the pentasaccharide lowering the dissociation constant for formation of the Michaelis-type noncovalent encounter complex.

As in its reaction with true substrates, the fXa catalytic residue, Ser-195, is required to form a covalent protease−serpin complex in the second step of the reaction. Thus, the inactive S195A mutant of fXa is expected to undergo only the first reaction step to form a reversible Michaelis-type complex with AT. To provide further support for the proposal that the primary role of pentasaccharide is to lower the dissociation constant for the formation of a noncovalent serpin−protease complex, the ability of the S195A mutant of GD-fXa to compete with wild-type GD-fXa for interaction with AT was evaluated in both the absence and presence of a fixed concentration of H5. As shown in Figure 3, the inactive fXa mutant effectively competed with its wild-type counterpart for interaction with AT in the presence of H5. Under these experimental conditions, S195A enzyme did not influence the reactivity of the wild-type enzyme in the absence of H5 (data not shown). Nonlinear regression analysis of data yielded a K_D of 255 ± 22 nM ($n = 6 \pm$ the standard deviation) for the interaction of the mutant fXa with the activated conformation of the serpin. These results clearly indicate that pentasaccharide improves the dissociation constant for formation of the noncovalent complex of fXa with AT. The ability to measure K_D for interaction of the mutant fXa with the AT−H5 complex by this approach was in apparent contradiction with the rapid kinetic approach in which no dissociation constant for the serpin−protease Michaelis-type complex could be measured for the AT−H5 complex up to 10 μM (Figure 1). To investigate this question

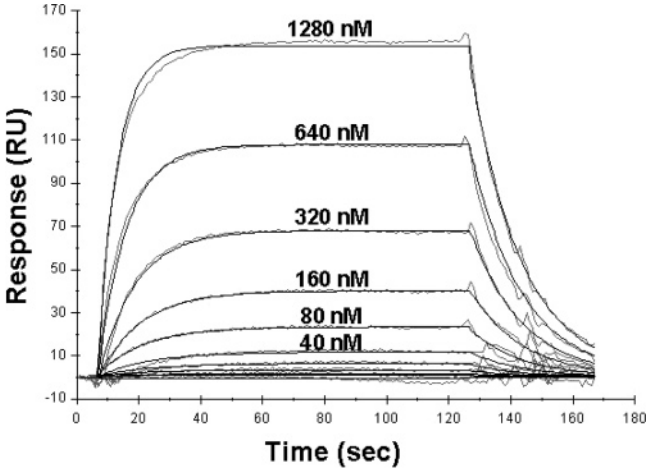

FIGURE 4: BIAcore sensogram for binding of the AT−H5 complex to the S195A mutant of GD-fXa. The fXa mutant was immobilized on a CM5 sensor chip followed by the injection of different concentrations of AT (2.5−1280 nM) diluted in the running buffer (HBS) containing 4 μM pentasaccharide as described in Materials and Methods. The rate constants for association (k_a) and dissociation (k_d) of the interaction of the AT−H5 complex with fXa were calculated from global fitting of the binding data (solid straight lines) to a 1:1 Langmuir binding model and presented in Scheme 1.

further, we evaluated the direct binding of S195A GD-fXa to AT by SPR analysis in both the absence and presence of H5. In agreement with the competition kinetic data, H5 lowered the K_D for the noncovalent interaction of AT with the mutant protease. As shown in Figure 4, AT interacted with the mutant protease with a K_D of 610 ± 70 nM in the presence of H5, whereas no interaction of AT with the protease was detected in the absence of pentasaccharide at the highest concentration of the serpin (Figure 4, baseline). SPR analysis yielded association (k_a) and dissociation (k_d) rate constants of (8.2 ± 0.3) × 10^4 M^{-1} s^{-1} and 0.05 ± 0.004 s^{-1}, respectively, for the interaction of the mutant fXa with the AT−H5 complex. Similar results were obtained in both TBS and HBS buffers. The reason for an ∼2-fold difference between K_D values as determined by either a competition kinetic or SPR approach is not known. Nevertheless, the results clearly indicate that the activation mechanism of AT involves H5 lowering the K_D for formation of a noncovalent serpin−protease encounter complex in the first step of the reaction.

The observation that the dissociation constant for interaction of the AT−H5 complex with the inactive S195A fXa could be determined by both competition kinetic and SPR approaches, but not for the interaction with wild-type fXa using the rapid kinetic method, may be explained by the Michaelis-type fXa−AT−H5 complex not establishing equilibrium at the initial binding step of the reaction. This kinetic behavior is characteristic for the reaction of enzymes with "sticky substrates" and occurs when the dissociation rate constant for the formation of a reversible Michaelis complex is slower than the rate constant for the subsequent formation of an acylated intermediate complex (*22*, *23*). Under these conditions, association of the enzyme with the substrate is diffusion-controlled and acylation is the rate-determining step in the reaction. This also appears to be the case for the reaction of fXa with the AT−H5 complex since as discussed below the rate of covalent complex formation is much faster

Scheme 1

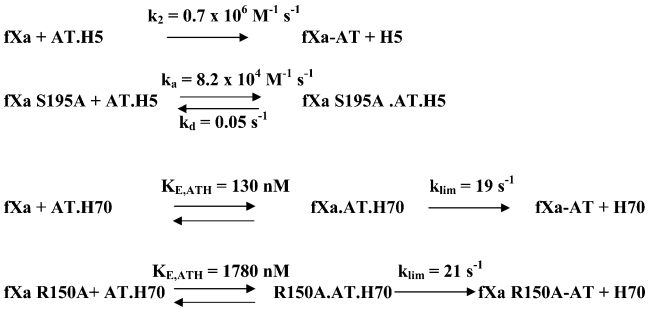

than the rate constant for dissociation of the noncovalent complex (k_d). The resolvable rate constants for the reaction of fXa with the AT−heparin complex determined in this study by either a rapid kinetic or SPR method are presented in Scheme 1.

Although it was not possible to resolve the two-step reaction of the AT−H5 complex with fXa, it is expected that the rate constant for formation of the stable covalent complex in this reaction will be higher than 19 s^{-1}, the rate constant for reaction of fXa with the AT−H70 complex. This contention is derived from the previous observation that in the absence of a template effect of heparin, fXa exhibits both high $K_{E,ATH}$ and k_{lim} values in reaction with the AT−heparin complex (*14*). Thus, previous rapid kinetic analysis has estimated a $K_{E,ATH}$ of ∼200 μM for the noncovalent reaction step and a limiting rate constant of 140 s^{-1} for reaction of fXa with AT in complex with a 26-saccharide high-affinity heparin in the absence of Ca^{2+} (*14*). Calcium affects the reactivity of fXa with AT in complex with a longer chain heparin by allowing the polysaccharide to bind to a basic exosite on fXa, thereby enhancing the reactivity of the protease with the serpin by a template mechanism (*12*, *24*). With the exception of its role in binding to the Gla domain and allowing the longer chain heparins to interact with a basic exosite of fXa (*24*), Ca^{2+} is not known to influence any other step of the AT−fXa reaction. In support of this proposal, fXa exhibits similar reactivity with the AT−H5 complex in both Ca^{2+} and EDTA (*13*), and under both experimental conditions, the Gla-domainless fXa reacts with the AT−H70 complex with $K_{E,ATH}$ and k_{lim} values similar to those obtained for wild-type fXa in the presence of Ca^{2+} (*13*). Thus, the rate constant for the covalent reaction step of fXa with the AT−H5 complex should approximate the same value (∼140 s^{-1}) reported for the reaction of fXa with AT in complex with 26-saccharide high-affinity heparin in EDTA (*14*). In this case, the rate constant of formation of the covalent complex is 2800-fold higher than the dissociation rate constant for formation of the noncovalent complex (k_d = 0.05 s^{-1}), as determined by SPR analysis. Because of such a large difference between reverse and forward rate constants, upon association of AT with the protease, the noncovalent complex is rapidly converted to a covalent complex without the establishment of equilibrium with free proteins. Under these conditions, the Michaelis-type complex [$K_{E,ATH} = (k_{lim} + k_d)/k_a = k_{lim}/k_a$] would not represent K_D and the rate of association of fXa and the AT−H5 complex would be diffusion-limited, with acylation being the rate-determining step in the reaction (*25*). This kinetic behavior can explain the inability of the rapid kinetic method to resolve the Michaelis constant for the noncovalent interaction of fXa

with the AT−H5 complex in the concentration ranges that were studied. On the other hand, in the case of the reaction of fXa with AT in complex with the longer chain heparin, the ability of heparin to simultaneously bind to both the serpin and the protease in the presence of Ca^{2+} dramatically lowers the dissociation constant for the noncovalent step at the expense of limiting the rate constant for the covalent step of the reaction. It is not known how the bridging function of heparin, mediated by Ca^{2+}, limits the rate of formation of the covalent protease−serpin complex. Nevertheless, it has been suggested that the bridging function of heparin may impede the conformational freedom of the serpin's trapping mechanism at the covalent step of the reaction (*25*, *26*). This reaction mechanism is analogous to that observed for the reaction of tissue plasminogen activator with plasminogen activator inhibitor-1. In this case, the interaction of a basic insertion loop of the protease with two negatively charged residues on the primed side of the reactive site loop of the serpin limits the rate constant for the acylation step of the reaction (*25*, *27*).

In summary, the results presented above, for the first time, demonstrate that pentasaccharide activates AT by decreasing the dissociation constant for the formation of a noncovalent encounter complex between AT and fXa in the first step of a two-step resolvable reaction. This was evidenced by the observation that (1) the equilibrium dissociation constant for formation of the ternary AT−heparin−fXa Michaelis-type complex was impaired by ∼1 order of magnitude for the R150A mutant of fXa, (2) the catalytically inactive S195A mutant of fXa effectively competed with wild-type fXa for binding to AT in the presence but not in the absence of H5, and (3) the SPR analysis suggested that AT can bind to S195A fXa only in the presence of H5.

ACKNOWLEDGMENT

I thank Dr. Steven Olson for critical reading and Audrey Rezaie for proofreading of the manuscript.

REFERENCES

1. Damus, P. S., Hicks, M., and Rosenberg, R. D. (1973) Anticoagulant action of heparin, *Nature 246*, 355−357.
2. Carrell, R. W., Stein, P. E., Fermi, G., and Wardell, M. R. (1994) Biological implications of a 3 Å structure of dimeric antithrombin, *Structure 2*, 257−270.
3. Olson, S. T., and Björk, I. (1992) Regulation of thrombin by antithrombin and heparin cofactor II, in *Thrombin: Structure and Function* (Berliner, L. J., Ed.) pp 159−217, Plenum Press, New York.
4. Bock, S. C., Wion, K. L., Vehar, G. A., and Lawn, R. M. (1982) Cloning and expression of the cDNA clone for human antithrombin III, *Nucleic Acids Res. 10*, 8113−8125.
5. Gettins, P. G. W. (2002) Serpins: Structure, mechanism, and function, *Chem. Rev. 102*, 4751−4803.
6. Huber, R., and Carrell, R. W. (1989) Implications of the three-dimensional structure of a1-antitrypsin for structure and function of serpins, *Biochemistry 28*, 8951−8966.
7. Jin, L., Abrahams, J., Skinner, R., Petitou, M., Pike, R. N., and Carrell, R. W. (1997) The anticoagulant activation of antithrombin by heparin, *Proc. Natl. Acad. Sci. U.S.A. 94*, 14683−14688.
8. Olson, S. T., Swanson, R., Raub-Segall, E., Bedsted, T., Sadri, M., Petitou, M., Herault, J. P., Herbert, J. M., and Björk, I. (2004) Accelerating ability of synthetic oligosaccharides on antithrombin inhibition of proteinases of the clotting and fibrinolytic systems. Comparison with heparin and low-molecular-weight heparin, *Thromb. Haemostasis 92*, 929−939.
9. Weitz, J. I., Hirsh, J., and Samama, M. M. (2004) New anticoagulant drugs: The seventh ACCP conference on antithrombotic and thrombolytic therapy, *Chest 126* (Suppl. 3), 265S−286S.
10. Olson, S. T., Björk, I., Sheffer, R., Craig, P. A., Shore, J. D., and Choay, J. (1992) Role of the antithrombin-binding pentasaccharide in heparin acceleration of antithrombin-proteinase reactions. Resolution of the antithrombin conformational change contribution to heparin rate enhancement, *J. Biol. Chem. 267*, 12528−12538.
11. Huntington, J. A., McCoy, A., Belzar, K. J., Pei, X. Y., Gettins, P. G. W., and Carrell, R. W. (2000) The conformational activation of antithrombin, *J. Biol. Chem. 275*, 15377−15383.
12. Rezaie, A. R. (1998) Calcium enhances heparin catalysis of the antithrombin-factor Xa reaction by a template mechanism. Evidence that calcium alleviates Gla-domain antagonism of heparin binding to factor Xa, *J. Biol. Chem. 273*, 16824−16827.
13. Rezaie, A. R., and Olson, S. T. (2000) Calcium enhances heparin catalysis of the antithrombin-factor Xa reaction by promoting the assembly of an intermediate heparin-antithrombin-factor Xa binding complex. Demonstration by rapid kinetics studies, *Biochemistry 39*, 12083−12090.
14. Craig, P. A., Olson, S. T., and Shore, J. D. (1989) Transient kinetics of heparin-catalyzed protease inactivation by antithrombin III: Characterization of assembly, product formation and heparin dissociation in the factor Xa reaction, *J. Biol. Chem. 264*, 5452−5461.
15. Olson, S. T., and Shore, J. D. (1982) Demonstration of a two-step reaction mechanism for inhibition of α-thrombin by antithrombin III and identification of the step affected by heparin, *J. Biol. Chem. 257*, 14891−14895.
16. Bode, W., Mayr, I., Baumann, U., Huber, R., Stone, S. R., and Hofsteenge, J. (1989) The refined 1.9 Å crystal structure of human α-thrombin: Interaction with D-Phe-Pro-Arg chloromethyl ketone and significance of the Tyr-Pro-Pro-Trp insertion segment, *EMBO J. 8*, 3467−3475.
17. Manithody, C., Yang, L., and Rezaie, A. R. (2002) Role of basic residues of the autolysis loop in the catalytic function of factor Xa, *Biochemistry 41*, 6780−6788.
18. Yang, L., Manithody, C., and Rezaie, A. R. (2004) Heparin-activated antithrombin interacts with the autolysis loop of target coagulation proteases, *Blood 104*, 1753−1759.
19. Rezaie, A. R., Neuenschwander, P. F., Morrissey, J. H., and Esmon, C. T. (1993) Analysis of the functions of the first epidermal growth factor-like domain of factor X, *J. Biol. Chem. 268*, 8176−8180.
20. Bock, P. E., Craig, P. A., Olson, S. T., and Singh, P. (1989) Isolation of human blood coagulation a-factor Xa by soybean trypsin inhibitor-sepharose chromatography and its active-site titration with fluorescein mono-p-guanidinobenzoate, *Arch. Biochem. Biophys. 273*, 375−388.
21. Olson, S. T., Björk, I., and Shore, J. D. (1993) Kinetic characterization of heparin-catalyzed and uncatalyzed inhibition of blood coagulation proteinases by antithrombin, *Methods Enzymol. 222*, 525−560.
22. Stone, S. R., Betz, A., and Hofsteenge, J. (1991) Mechanistic studies on thrombin catalysis, *Biochemistry 30*, 9841−9848.
23. Hopfner, K.-P., and Di Cera, E. (1992) Energetics of thrombin-fibrinogen interaction, *Biochemistry 31*, 11567−11571.
24. Rezaie, A. R. (2000) Identification of basic residues in the heparin-binding exosite of factor Xa critical for heparin and factor Va binding, *J. Biol. Chem. 275*, 3320−3327.
25. Olson, S. T., Swanson, R., Day, D., Verhamme, I., Kvassman, J., and Shore, J. D. (2001) Resolution of Michaelis complex, acylation, and conformational change steps in the reactions of the serpin, plasminogen activator inhibior-1, with tissue plasminogen activator and trypsin, *Biochemistry 40*, 11742−11756.
26. Chuang, Y.-J., Gettins, P. G. W., and Olson, S. T. (1999) Importance of the P2 glycine of antithrombin in target proteinase specificity, heparin activation, and the efficiency of proteinase trapping as revealed by a P2 Gly to Pro mutation, *J. Biol. Chem. 274*, 28142−28149.
27. Kvassman, J.-O., Verhamme, I., and Shore, J. D. (1998) Inhibitory mechanism of serpins: Loop insertion forces acylation of plasminogen activator by plasminogen activator inhibitor-1, *Biochemistry 37*, 15491−15502.

BI060056R